REPORT DOCUMENTATION PAGE

Form Approved OMB NO. 0704-0188

The public reporting burden for this collection of information is estimated to average 1 hour per response, including the time for reviewing instructions, searching existing data sources, gathering and maintaining the data needed, and completing and reviewing the collection of information. Send comments regarding this burden estimate or any other aspect of this collection of information, including suggesstions for reducing this burden, to Washington Headquarters Services, Directorate for Information Operations and Reports, 1215 Jefferson Davis Highway, Suite 1204, Arlington VA, 22202-4302. Respondents should be aware that notwithstanding any other provision of law, no person shall be subject to any oenalty for failing to comply with a collection of information if it does not display a currently valid OMB control number.
PLEASE DO NOT RETURN YOUR FORM TO THE ABOVE ADDRESS.

1. REPORT DATE (DD-MM-YYYY)	2. REPORT TYPE	3. DATES COVERED (From - To)
11-12-2015	Final Report	11-Jul-2014 - 10-Feb-2016

4. TITLE AND SUBTITLE

Final Report: Koopman Mode Decomposition Methods in Dynamic Stall: Reduced Order Modeling and Control

5a. CONTRACT NUMBER

5b. GRANT NUMBER

W911NF-14-C-0102

5c. PROGRAM ELEMENT NUMBER

611102

6. AUTHORS

Maria Fonoberova, Igor Mezic, Sophie Loire

5d. PROJECT NUMBER

5e. TASK NUMBER

5f. WORK UNIT NUMBER

7. PERFORMING ORGANIZATION NAMES AND ADDRESSES

AIMdyn, Inc
1919 State St, suite 207

Santa Barbara, CA 93101 -8455

8. PERFORMING ORGANIZATION REPORT NUMBER

9. SPONSORING/MONITORING AGENCY NAME(S) AND ADDRESS (ES)

U.S. Army Research Office
P.O. Box 12211
Research Triangle Park, NC 27709-2211

10. SPONSOR/MONITOR'S ACRONYM(S)

ARO

11. SPONSOR/MONITOR'S REPORT NUMBER(S)

65502-EG.3

12. DISTRIBUTION AVAILIBILITY STATEMENT

Approved for Public Release; Distribution Unlimited

13. SUPPLEMENTARY NOTES

The views, opinions and/or findings contained in this report are those of the author(s) and should not contrued as an official Department of the Army position, policy or decision, unless so designated by other documentation.

14. ABSTRACT

During dynamic stall, large peaks in lift, pitching moment and drag appear, and these cause an undesirable increase in the mean drag. Dynamic stall can also lead to potentially fatal structural loads due to strong vibrations of flexible aerodynamic surfaces. Despite extensive analytical, numerical, and experimental efforts to study dynamic stall, progress is needed for the full
understanding and prediction of the relevant complex fluid dynamic mechanisms.

15. SUBJECT TERMS

Koopman Mode Decomposition, Reduced Order Modeling and Control

16. SECURITY CLASSIFICATION OF:			17. LIMITATION OF ABSTRACT	15. NUMBER OF PAGES	19a. NAME OF RESPONSIBLE PERSON
a. REPORT	b. ABSTRACT	c. THIS PAGE			Maria Fonoberova
UU	UU	UU	UU		19b. TELEPHONE NUMBER 805-687-6999

Report Title

Final Report: Koopman Mode Decomposition Methods in Dynamic Stall: Reduced Order Modeling and Control

ABSTRACT

During dynamic stall, large peaks in lift, pitching moment and drag appear, and these cause an undesirable increase in the mean drag. Dynamic stall can also lead to potentially fatal structural loads due to strong vibrations of flexible aerodynamic surfaces. Despite extensive analytical, numerical, and experimental efforts to study dynamic stall, progress is needed for the full understanding and prediction of the relevant complex fluid dynamic mechanisms.

We propose to do the following:
1. Continue the research on cylinder in an oscillating incoming flow that is proving to be a useful "model system". We will include effects of oscillation of direction of incoming velocity vector (and not just its magnitude) to emulate effects of separation at the leading edge.
2. Explore an analytical direction by extending the Ginzburg-Landau equation approach to compute Koopman Modes for flow around the cylinder with oscillating incoming velocity and compare with numerical approach. This will be done in collaboration with ARL.
3. Explore Koopman Mode Decomposition in 2-D and 3-D data of plunging airfoil provided by Dr. Miguel Visbal of AFRL.
4. Provide a Reduced Order Model (ROM) of Dynamic Stall using skew-projection methods in conjunction with the Koopman Mode Decomposition.

Enter List of papers submitted or published that acknowledge ARO support from the start of the project to the date of this printing. List the papers, including journal references, in the following categories:

(a) Papers published in peer-reviewed journals (N/A for none)

Received Paper

TOTAL:

Number of Papers published in peer-reviewed journals:

(b) Papers published in non-peer-reviewed journals (N/A for none)

Received Paper

TOTAL:

Number of Papers published in non peer-reviewed journals:

(c) Presentations

Koopman decompositions of periodically forced Hopf bifurcation flows and application to dynamic stall. 68th Annual Meeting of the APS Division of Fluid Dynamics. Volume 60, Number 21. Sunday–Tuesday, November 22–24, 2015; Boston, Massachusetts. Authors: Bryan Glaz (U.S. Army Research Laboratory), Sophie Loire (Aimdyn, Inc.), Maria Fonoberova (Aimdyn, Inc.), Igor Mezic (University of California Santa Barbara).

Periodically forced Hopf bifurcation flows, such as oscillating cylinders, can exhibit rich spectral content. Though lock-on dynamics of systems forced near resonances are well understood, the underlying chaotic or quasi-periodic dynamics when forcing away from a natural frequency are not. This behavior can be critical for systems of practical significance, such as oscillating airfoils under dynamic stall. In this study, normal form theory and spectral decompositions based on Koopman operators will be used to reveal transitions from limit cycle attractors to chaotic/quasi-periodic dynamics in the cylinder Hopf bifurcation flow. Koopman operator methods are used since each mode is associated with a single frequency which allows one to observe the evolution to more continuous spectral behavior with forcing, while approaches such as proper orthogonal decomposition may obfuscate this transition. It will be shown that projecting onto a low order subspace of Koopman modes can capture features supported by normal forms. Using this, we show a mechanism that leads to regimes in which the system seems to exhibit shear-induced chaos. The new framework is applied to dynamic stall studies to establish periodically forced Hopf bifurcation dynamics as an underlying feature.

Number of Presentations: 1.00

Non Peer-Reviewed Conference Proceeding publications (other than abstracts):

Received	Paper

TOTAL:

Number of Non Peer-Reviewed Conference Proceeding publications (other than abstracts):

Peer-Reviewed Conference Proceeding publications (other than abstracts):

Received	Paper	
07/02/2015	1.00	Bryan Glaz, Maria Fonoberova, Sophie Loire, Igor Mezic. Analysis of Fluid Motion in Dynamic Stall and Forced Cylinder Flow Using Koopman Operator Methods, ASME 2014 International Mechanical Engineering Congress and Exposition. 14-NOV-14, Montreal, Quebec, Canada. : ,

TOTAL: **1**

Number of Peer-Reviewed Conference Proceeding publications (other than abstracts):

(d) Manuscripts

Received Paper

TOTAL:

Number of Manuscripts:

Books

Received Book

TOTAL:

Received Book Chapter

TOTAL:

Patents Submitted

Patents Awarded

Awards

Graduate Students

NAME	PERCENT_SUPPORTED

FTE Equivalent:
Total Number:

Names of Post Doctorates

NAME	PERCENT_SUPPORTED

FTE Equivalent:
Total Number:

Names of Faculty Supported

NAME	PERCENT_SUPPORTED

FTE Equivalent:
Total Number:

Names of Under Graduate students supported

NAME	PERCENT_SUPPORTED

FTE Equivalent:
Total Number:

Student Metrics

This section only applies to graduating undergraduates supported by this agreement in this reporting period

The number of undergraduates funded by this agreement who graduated during this period: 0.00

The number of undergraduates funded by this agreement who graduated during this period with a degree in science, mathematics, engineering, or technology fields:..... 0.00

The number of undergraduates funded by your agreement who graduated during this period and will continue to pursue a graduate or Ph.D. degree in science, mathematics, engineering, or technology fields:..... 0.00

Number of graduating undergraduates who achieved a 3.5 GPA to 4.0 (4.0 max scale):..... 0.00

Number of graduating undergraduates funded by a DoD funded Center of Excellence grant for Education, Research and Engineering:..... 0.00

The number of undergraduates funded by your agreement who graduated during this period and intend to work for the Department of Defense 0.00

The number of undergraduates funded by your agreement who graduated during this period and will receive scholarships or fellowships for further studies in science, mathematics, engineering or technology fields: 0.00

Names of Personnel receiving masters degrees

NAME

Total Number:

Names of personnel receiving PHDs

NAME
Total Number:

Names of other research staff

NAME	PERCENT_SUPPORTED
Maria Fonoberova	0.70
Igor Mezic	0.20
Sophie Loire	0.20
FTE Equivalent:	**1.10**
Total Number:	**3**

Sub Contractors (DD882)

Inventions (DD882)

Scientific Progress

See Attachment

Technology Transfer

Project Title: Koopman Mode Decomposition Methods in Dynamic Stall: Reduced Order Modeling and Control
Contract Number: W911NF-14-C-0102
Proposal Number: P-65502-EG
Period: July 11, 2014 – November 10, 2015
PI: Dr. Maria Fonoberova
Institution: AIMdyn, Inc.

Final Technical Report

Introduction

High manoeuvrability requirements on modern helicopters require the necessity of deeper understanding of dynamics, and in turn possibilities for control of, dynamic stall. Unsteady flow and resulting aerodynamic loads strongly affect the propulsive efficiency of highly loaded helicopter rotor blades [Ham:1968], [Johnson:1972]. Thus, there is currently much interest in the unsteady aerodynamics of flows relevant to rotorcraft (manned and unmanned) air vehicles. The flowfields in these applications exhibit unsteady separation followed by the formation of dynamic-stall-like vortices whose evolution and interaction with flexible aerodynamic surfaces have a significant impact on flight stability and performance and in turn on structural design [Barwey:1994]. Analysis of these flows is complicated further by their mixed laminar transitional turbulent character at moderate Reynolds numbers, as well as by the broad range of possible parameters, kinematics, and configurations. To facilitate progress in the understanding and prediction of the relevant fluid dynamic mechanisms, it is natural to consider methods that provide simplification of the flow phenomena by separating them into individual modes. The technique of Proper Orthogonal Decomposition (POD), see [Holmes: 1998] is a popular way of accomplishing this task. However, while POD is capable of extracting the most energetic parts of the flow field, it has been shown to lack ability of highlighting subtle, oscillatory phenomena that are nevertheless implicated in important physical processes such as the shear layer separation.

Unsteady flows over plunging and pitching airfoils with large excursions in effective angle of attack exhibit the phenomenon termed dynamic stall, a process characterized phenomenologically by unsteady separation and by the formation of large-scale leading-edge and trailing-edge vortices, which exert difficult-to-predict variations in aerodynamic loads. Distinct stages of the evolution of dynamic stall are a) vortex formation, b) vortex convection, c) stall onset and d) stalled stage. Comprehensive reviews of this phenomenon, first discovered and studied extensively in the context of helicopter rotor blades, has been given by McCroskey [Mccroskey:1982], [Carr:2012], and [Ekaterinaris:1998].

Aimdyn and AFRL have been studying physical mechanisms of dynamic stall using the methods of Koopman operator theory. The initial seed research has suggested existence of high-frequency effects in leading edge vortex shedding events, not present in the static stall case. The research guided by dynamical systems methods and efficient numerical methods for Koopman Mode Decomposition already lead to interesting outcomes. Among those are insight into the physical effects of the oscillatory nature of the incoming velocity that the wing experiences due to pitch or plunging. For example, the examination of a model system - a cylinder in an incoming oscillatory flow - showed some of the physical effects (e.g. broadening of the spectrum) observed in the pitching airfoil case are present in the model system and shed light on the dynamics of aspects of pitching airfoil dynamics as a nonlinear interaction of the forcing by the oscillating incoming flow frequency and natural frequency of vortex shedding dynamics. In collaboration with the Army Research Laboratory's Dr. Bryan Glaz, we found the precise state-space description of the mechanism of the broadening of the spectrum by examining perturbations of the limit cycling motion by external forcing frequency.

Koopman Modes for Stationary Airfoil with Different Degrees of Oscillation Amplitude

Koopman mode decomposition is based on the surprising fact, discovered in [Mezic: 2005], that normal modes of linear oscillations have its natural analogue - Koopman modes - in the context of nonlinear dynamics. To pursue this analogy, one must change the representation of the system from the state-space representation to the dynamics governed by the linear Koopman operator ([Koopman: 1931]) on an infinite-dimensional space of observables. Contrary to the proper orthogonal decomposition, the dynamic mode decomposition contains not only information about coherent structures, but also about their temporal evolution.

Based on snapshots of the flow, we can approximate the Koopman Modes using an Arnoldi-like algorithm sometimes called dynamic mode decomposition (DMD) ([Schmid: 2008], [Rowley: 2009]) which computes eigenvalues based on the so-called companion matrix.

Given a sequence of equispaced in time snapshots from numerical simulations or physical experiments, with Δt being the time interval between snapshots, a data matrix is formed with columns that represent the individual data samples $u_j \in R^n, j = 0, \dots, m$, with j representing time $j\Delta t$. The companion matrix is then defined as:

$$C = \begin{pmatrix} 0 & 0 & \cdots & 0 & c_0 \\ 1 & 0 & & 0 & c_1 \\ 0 & 1 & & 0 & c_2 \\ \vdots & & \ddots & & \vdots \\ 0 & 0 & \cdots & 1 & c_{m-1} \end{pmatrix}$$

where $c_i, i = 0, \dots, m-1$ are such that:

$$u_m = \sum_{j=0}^{m-1} c_i u_i + r$$

and r is the residual vector.

The spectrum of the Koopman operator restricted to the subspace spanned by u_j is equal to the spectrum of the infinite-dimensional companion matrix and the associated Koopman modes are

given by Ka (provided that a does not belong to the null space of K), where $K = [u_0, u_1, \dots, u_{m-1}]$ is the column matrix (vector-valued) of observables snapshots at times $0, \Delta t, \dots, (m-1)\Delta t$ and a is an eigenvector of the shift operator restricted to Krylov subspace spanned by u_i which the Companion matrix is an approximation of. The approximate Koopman eigenvalues and eigenvectors obtained by the Arnoldi's algorithm are called Ritz eigenvalues and eigenvectors.

The standard Arnoldi-type algorithm to calculate the Ritz eigenvalues λ_j and eigenfunctions v_j is as follows:

1. Define $K = [u_0, u_1, \dots, u_{m-1}]$.

2. Find constants c_j such that:

$$r = u_m - \sum_{j=0}^{m-1} c_j u_j = u_m - Kc,\ r \perp span\{u_0, \dots, u_{m-1}\}.$$

This can be done by defining $c = K^{+}u_m$, where K^{+} is the pseudo inverse of K.

3. Define the companion matrix C as above and find its eigenvalues and eigenvectors:

$$C = T^{-1}\Lambda T, \Lambda = diag(\lambda_1, \cdots, \lambda_m),$$

where eigenvectors are columns of T^{-1}. Note that the Vandermonde matrix $\tilde{T}$

$$\tilde{T} = \begin{pmatrix} 1 & \lambda_1 & \lambda_1^2 & \cdots & \lambda_1^{m-1} \\ 1 & \lambda_2 & \lambda_2^2 & \cdots & \lambda_2^{m-1} \\ \vdots & \vdots & \vdots & \ddots & \vdots \\ 1 & \lambda_m & \lambda_m^2 & \cdots & \lambda_m^{m-1} \end{pmatrix}$$

diagonalizes the companion matrix C , as long as the eigenvalues $\lambda_1, \dots, \lambda_m$ are distinct.

4. Define v_j to be the columns of $V = K\tilde{T}^{-1}$.

Then, the Arnoldi-type Koopman Mode Decomposition gives:

$$\forall k = [0, 1, \cdots, m],\ u_k = \sum_{j=1}^{m} \lambda_j^k V(:, j)$$

We studied the stationary airfoil simulation provided by our collaborator Dr. Bryan Glaz at the U.S. Army Research Laboratory. The simulation was for a statically pitched NACA 0015 airfoil. The airfoil chord was 0.135 m, fresstream velocity magnitude was 100 m/s, and the freestream was oriented at a static 18 degree angle of attack. We also studied the case with 6 deg oscillation amplitude as well as 2 deg, 4 deg and 8 deg oscillation amplitude.

Figure 1 shows Fourier and KMD spectrum for u-velocity.

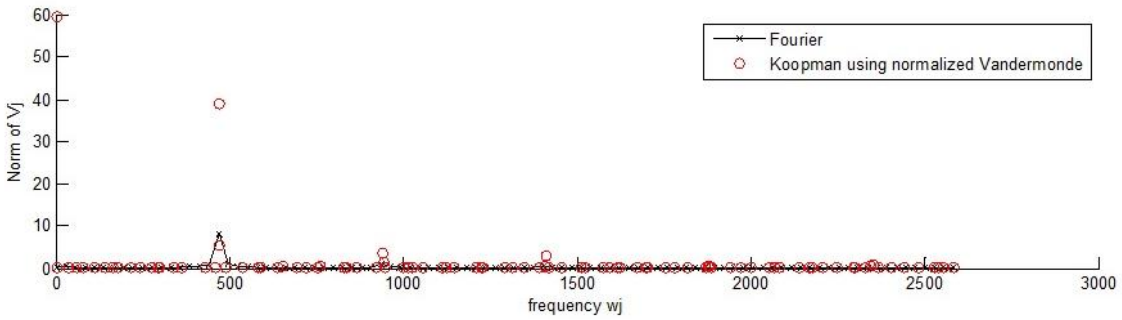

Figure 1. Fourier and KMD spectrum. FFT is in black; KM spectrum is red.

The obtained Koopman mode eigenvalues are shown in Figure 2, DMD spectrum in frequency w, exponential rate mu plane is shown in Figure 3.

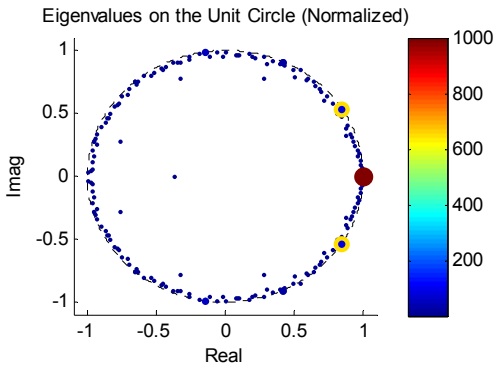

Figure 2. Koopman Mode Eigenvalues.

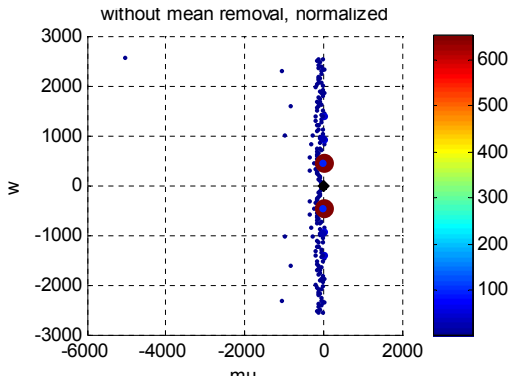

Figure 3. DMD spectrum in frequency w, exponential rate mu plane.

The recomposition of signal using 40 first pairs of the highest magnitude modes sorted by abs of norm of Vj has been performed. Figure 4 shows the reconstructed signal (red) vs the original data (blue).

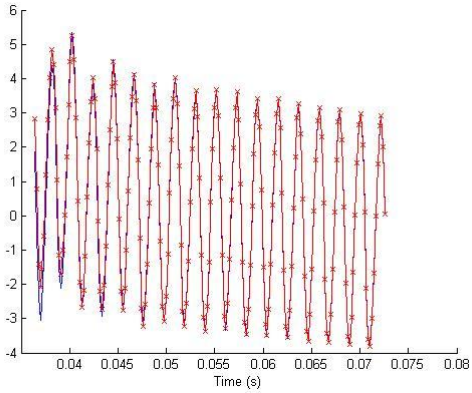

Figure 4. The reconstructed signal (red) vs the original data (blue) for the random location.

Magnitude, phase, real part and imaginary part for the Koopman mode corresponding to frequency 470 Hz are shown in Figure 5.

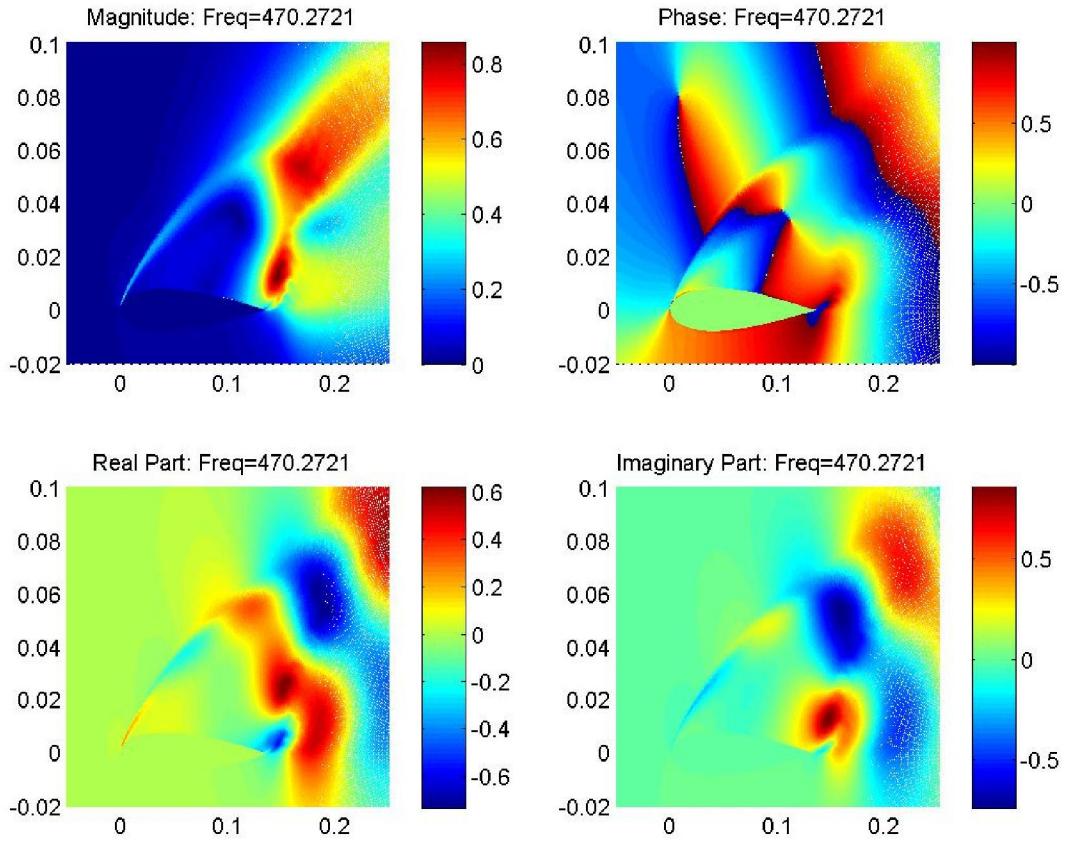

Figure 5. Magnitude, phase, real part and imaginary part for the Koopman mode corresponding to frequency 470 Hz.

Figure 6 shows Fourier and KMD spectrum for u-velocity for the airfoil case with 6 deg oscillation amplitude.

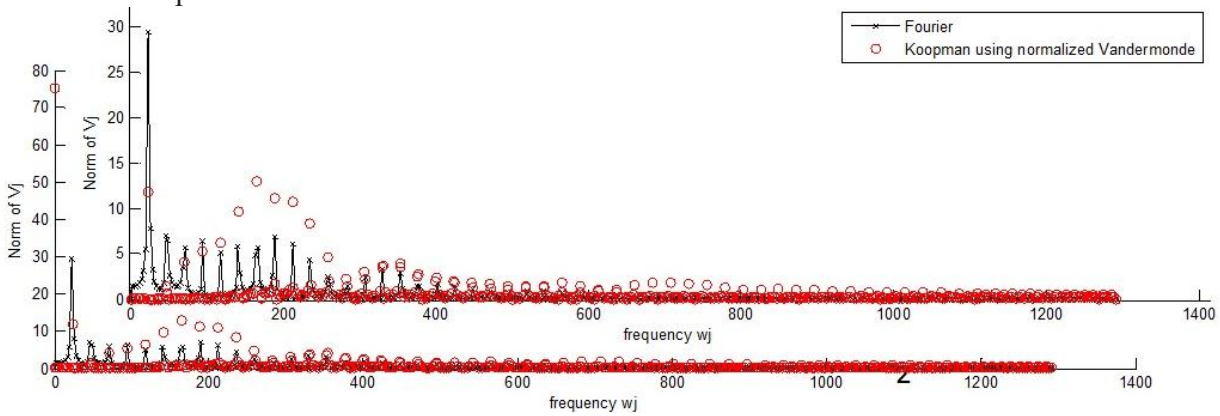

Figure 6. Fourier and KMD spectrum for the airfoil case with 6 deg oscillation amplitude. FFT is in black; KM spectrum is red.

Figure 7 shows Fourier and KMD spectrum for u-velocity for the airfoil case with 2 deg oscillation amplitude.

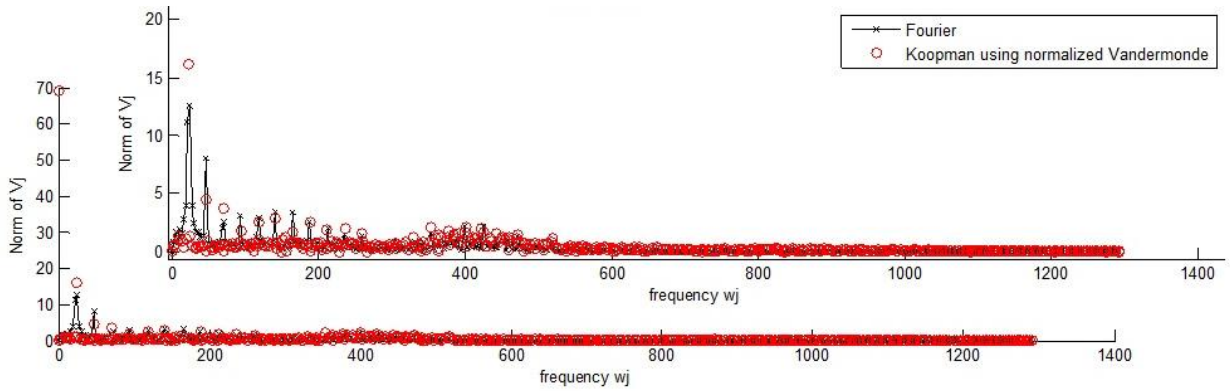

Figure 7. Fourier and KMD spectrum for the airfoil case with 2 deg oscillation amplitude. FFT is in black; KM spectrum is red.

Figure 8 shows Fourier and KMD spectrum for u-velocity for the airfoil case with 4 deg oscillation amplitude.

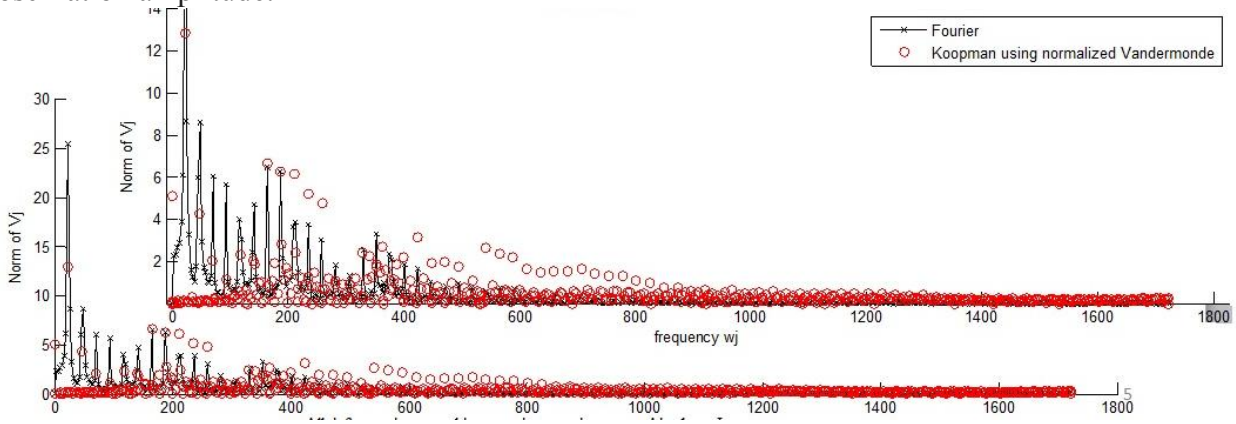

Figure 8. Fourier and KMD spectrum for the airfoil case with 4 deg oscillation amplitude. FFT is in black; KM spectrum is red.

The real part for the Koopman mode corresponding to frequency 24 Hz for the u-velocity for the airfoil case with 6 deg oscillation amplitude is shown in Figure 9A, the real part for the Koopman mode corresponding to frequency 23.5 Hz for the u-velocity for the airfoil case with 2 deg oscillation amplitude is shown in Figure 9B, the real part for the Koopman mode corresponding to frequency 23.5 Hz for the u-velocity for the airfoil case with 4 deg oscillation amplitude is shown in Figure 9C.

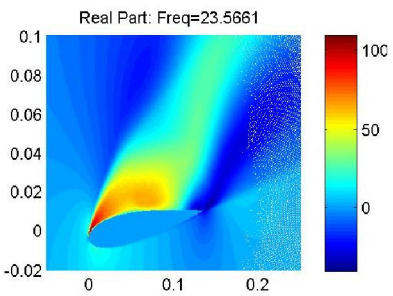

Figure 9A. The real part for the Koopman mode corresponding to frequency 23.5 Hz for the airfoil case with 6 deg oscillation amplitude.

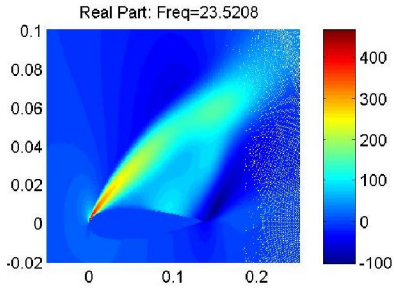

Figure 9B. The real part for the Koopman mode corresponding to frequency 23.5 Hz for the airfoil case with 2 deg oscillation amplitude.

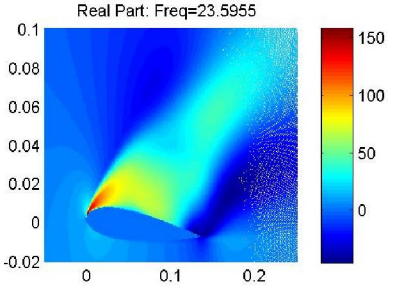

Figure 9C. The real part for the Koopman mode corresponding to frequency 23.5 Hz for the airfoil case with 4 deg oscillation amplitude

Connection between a basic version of the dynamic mode decomposition and the discrete-time version of the generalized Laplace analysis

We studied the connection between a basic version of the dynamic mode decomposition and the discrete-time version of the generalized Laplace analysis to apply to the airfoil case.

Theorem: Let f(x;z) be a field of observables f(x;z) : M x A -> R^m, where the observables are indexed over the set A. We will occasionally drop the dependence on the state-space variable x and denote f(x;z) = f(z) and the iterates of f by $f(T^i x;z) = f^i(z)$. Let $\lambda_0, ..., \lambda_k$ be the eigenvalues of U^t such that $||\lambda_0|| \geq ||\lambda_1|| \geq \ \ldots \geq ||\lambda_k||$. Then, the Koopman mode associated with λ_k is obtained by computing

$$f_k = \varphi_k(x)s_k(z) = \lim_{n\to\infty} \frac{1}{n}\sum_{i=0}^{n-1} \lambda_k^{-i}\left(f(T^i x, z) - \sum_{j=0}^{k-1} \lambda_j^i \varphi_j(x)s_j(z)\right),$$

$$= \lim_{n\to\infty} \frac{1}{n}\sum_{i=0}^{n-1} \lambda_k^{-i}\left(f^i(z) - \sum_{j=0}^{k-1} \lambda_j^i f_j\right),$$

We showed an explicit relationship between a basic version of the Dynamic Mode Decomposition (DMD) and the Koopman Mode Decomposition (KMD) of dynamical systems, that allows for estimates of validity of approximation of Koopman modes by DMD modes. We also linked the recently introduced Generalized Laplace Analysis and the inverse of the Vandermonde matrix. We proved the equivalence between dynamic modes and Koopman modes over infinite iteration of the dynamical system.

Prony Methods

We also studied Prony methods [Plonka: 2014] for recovery of structured functions and implemented the following algorithm in C++.

Algorithm (Classical Prony method)

Input:
M ⊆ N, sampled values h(k), k = 0,…,2M-1, of the exponential sum

$$h(x) := \sum_{j=1}^{M} c_j \, \mathrm{e}^{f_j x}, \quad x \geq 0,$$

1. Solve the following linear system

$$\mathbf{H}_M(0) \, (p_k)_{k=0}^{M-1} = -\big(h(M+m)\big)_{m=0}^{M-1}$$

where

$$\mathbf{H}_M(0) := \begin{pmatrix} h(0) & h(1) & \dots & h(M-1) \\ h(1) & h(2) & \dots & h(M) \\ \vdots & \vdots & & \vdots \\ h(M-1) & h(M) & \dots & h(2M-2) \end{pmatrix} = \big(h(k+m)\big)_{k,m=0}^{M-1}.$$

2. Compute all zeros $z_j \subseteq D$, j = 1,…,M, of the Prony polynomial

$$p(z) := \prod_{j=1}^{M} (z - z_j) = \sum_{k=0}^{M-1} p_k \, z^k + z^M, \quad z \in \mathbb{C}$$

i.e., calculate all eigenvalues of the associated companion matrix

$$\mathbf{C}_M(p) := \begin{pmatrix} 0 & 0 & \dots & 0 & -p_0 \\ 1 & 0 & \dots & 0 & -p_1 \\ 0 & 1 & \dots & 0 & -p_2 \\ \vdots & \vdots & & \vdots & \vdots \\ 0 & 0 & \dots & 1 & -p_{M-1} \end{pmatrix}.$$

and form $f_j = \log z_j$ for j = 1,…,M, where log is the principal value of the complex logarithm.
3. Solve the Vandermonde system

$$\mathbf{V}_M(\mathbf{z}) \, (c_j)_{j=1}^{M} = (h(k))_{k=0}^{M-1}.$$

Output:

$f_j \in [-\alpha, 0] + \mathrm{i}\,[-\pi, \pi)$, $c_j \in \mathbb{C}$, $j = 1, \dots, M$.

Bifurcation around a Critical Reynold's Number

We were looking at the theoretical explanation of our numeric observations of bifurcation around a critical Reynold's number. Reading paper [Bagheri: 2013], we realized that we could look at this issue as a forced oscillator set up similar to the one in paper [Vance: 1989]. We were studying this paper to apply the theory to our case.

We compared analytic solutions for the bifurcation sets of the truncated normal form of the dynamic equations for p=1 (Figure 10A), p=2 (Figure 10B) and p=40 (Figure 10C).

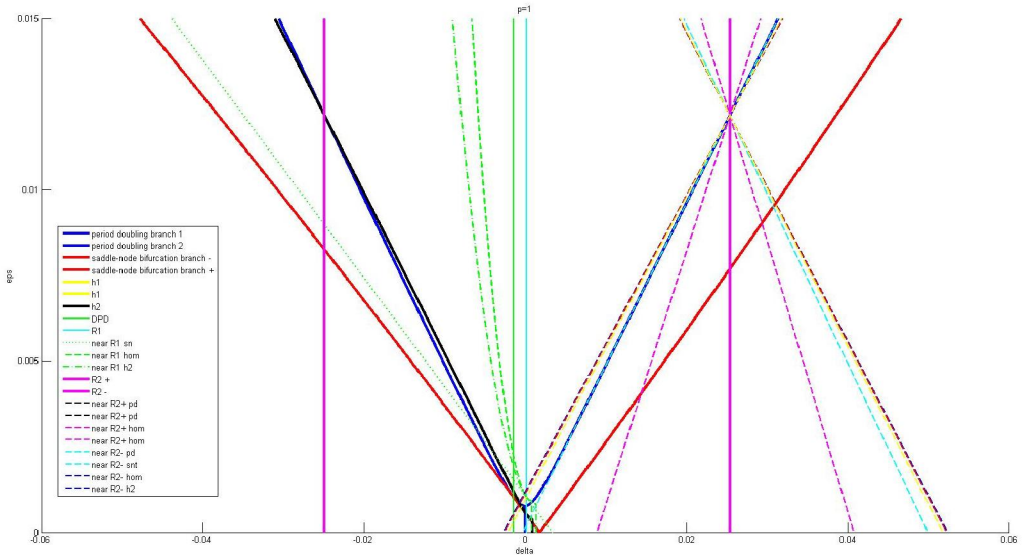

Figure 10A. p=1

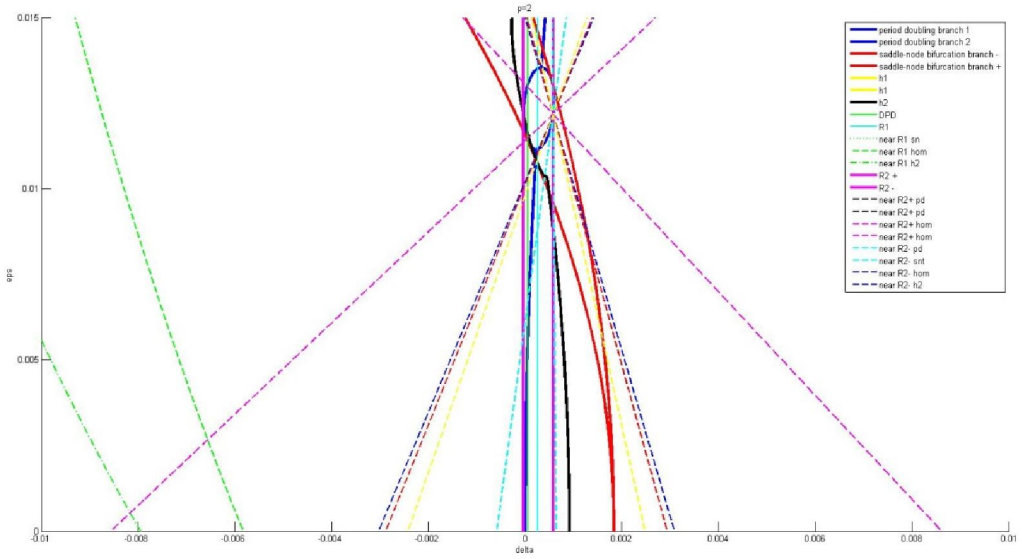

Figure 10B. p=2

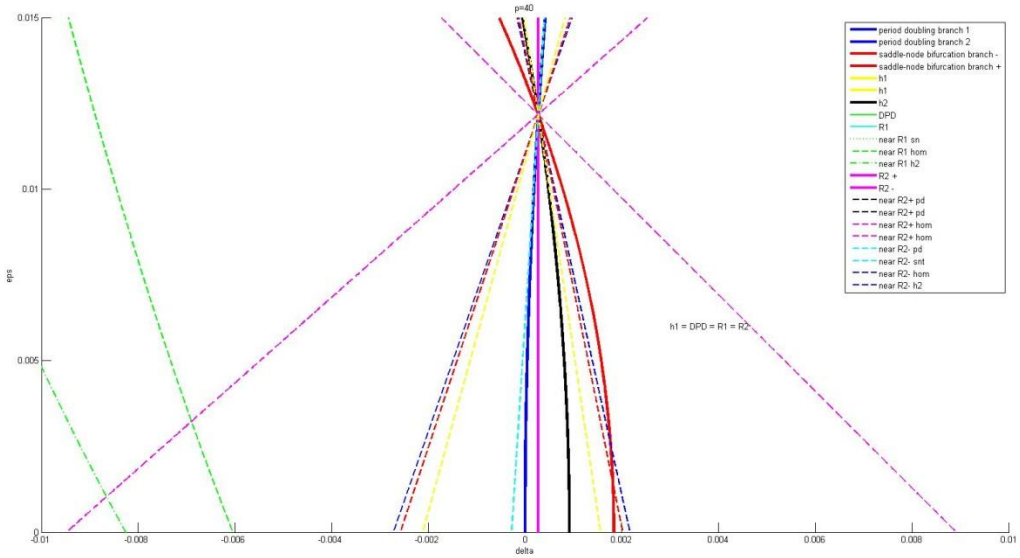

Figure 10C. p=40

We researched the following papers: [Wang: 2003], [Lin: 2008]. The main idea there is that for large periods T of perturbation chaotic behavior arises in systems with Hopf bifurcation. This is a restricted result in that the considered perturbation consists of kicks. We are considering pursuing simulations of a simple system where the perturbation is smooth, and pursuing CFD with oscillating forcing in form of kicks with very large period.

The team members studied the cylinder wake simulation provided by our collaborator Dr. Bryan Glaz at the U.S. Army Research Laboratory. There are two cases for p=1 and for p=2 (assuming q=2 in the paper [Vance: 1989]). For p=1 the cylinder is oscillated at twice the natural bifurcation frequency, and at p=2 it is oscillated at the natural shedding frequency of ~39 Hz. Within each p, there are large amplitude oscillation and small amplitude oscillation. For p=2, the tecplot output files were output at every 12 time steps (CFD time step size = 1e-4 s). The first 5000 time steps and the corresponding output files are for the stationary cylinder. Then, the cylinder is oscillated for the remaining time steps. After 5000 time steps, each case is run enough time to capture about 10-12 periods of the oscillation frequency. Everything the same is for p=1, except files are outputted at every 6 time steps. It was done because the cylinder oscillates twice as fast as the p=2 case and to make sure to capture higher frequency content.

Figure 11 shows Fourier and KMD spectrum for u-velocity for p=1 and small amplitude.

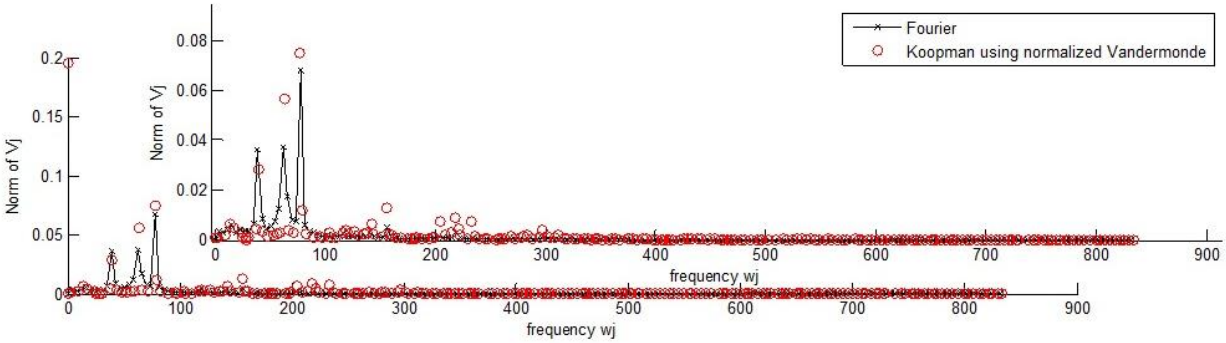

Figure 11. Fourier and KMD spectrum. FFT is in black; KM spectrum is red.

The obtained Koopman mode eigenvalues are shown in Figure 12, DMD spectrum in frequency w, exponential rate mu plane is shown in Figure 13.

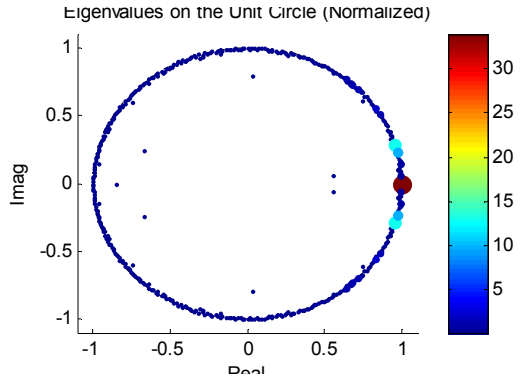

Figure 12. Koopman Mode Eigenvalues.

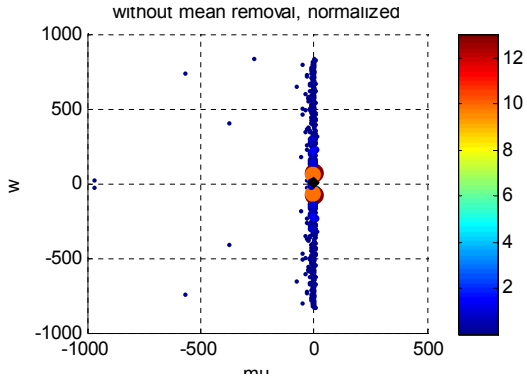

Figure 13. DMD spectrum in frequency w, exponential rate mu plane.

The recomposition of signal using 20 first pairs of the highest magnitude modes sorted by abs of norm of Vj has been performed. Figure 14 shows the reconstructed signal (red) vs the original data (blue).

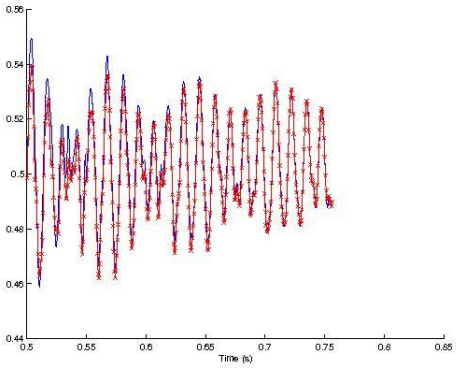

Figure 14. The reconstructed signal (red) vs the original data (blue) for the random location.

Figure 15 shows Fourier and KMD spectrum for u-velocity for p=2 and small amplitude by using not-normalized Vandermonde matrix (top) and normalized Vandermonde matrix (bottom).

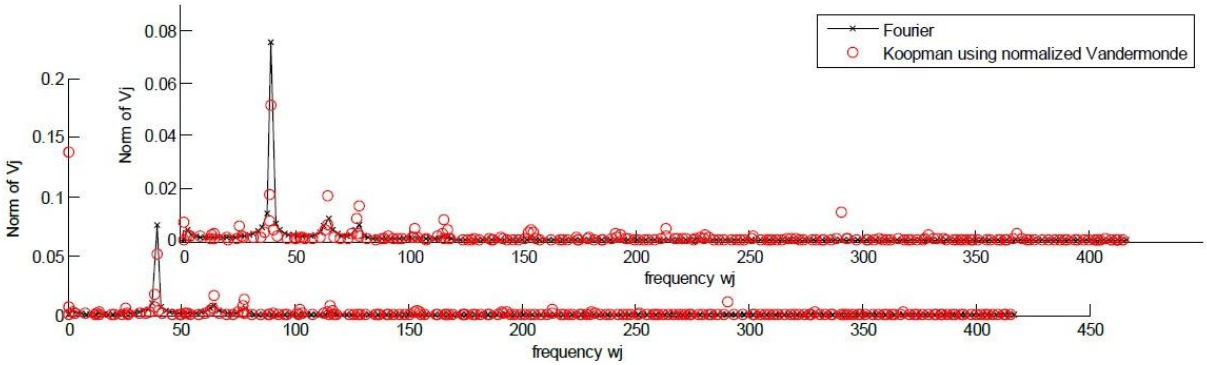

Figure 15. Fourier and KMD spectrum. FFT is in black; KM spectrum is red.

The obtained Koopman mode eigenvalues are shown in Figure 16, DMD spectrum in frequency w, exponential rate mu plane is shown in Figure 17.

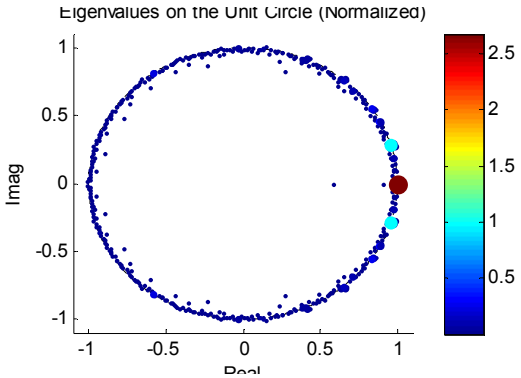

Figure 16. Koopman Mode Eigenvalues.

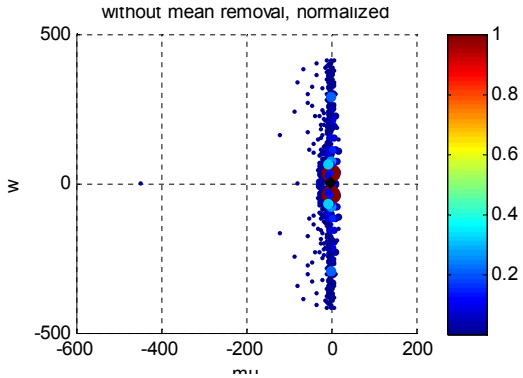

Figure 17. DMD spectrum in frequency w, exponential rate mu plane.

The recomposition of signal using 20 first pairs of the highest magnitude modes sorted by abs of norm of Vj has been performed. Figure 18 shows the reconstructed signal (red) vs the original data (blue).

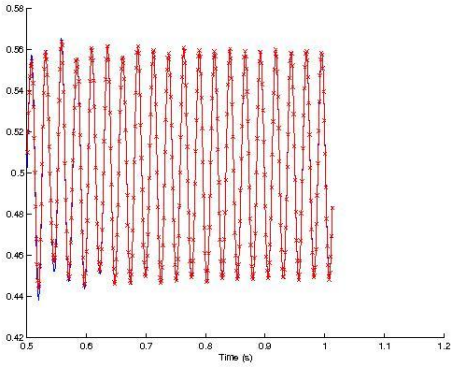

Figure 18. The reconstructed signal (red) vs the original data (blue) for the random location.

Reduced Order Model (ROM) of Dynamic Stall

The team members began working on the Reduced Order Model (ROM) of Dynamic Stall using skew-projection methods used in conjunction with the Koopman Mode Decomposition.

We used the following four cylinder simulations provided by Dr. Bryan Glaz at the U.S. Army Research Laboratory. The cylinder was 0.002m in diameter. Each simulation was run for 6 s. The number of nodes in the grid is 29954. For the stationary cylinder case, there are output files at every 12 time steps, so the delta t between outputs is 0.0012 s. For the oscillating cylinder cases, flow snapshots were outputted starting at the 25th time step, up to the 60,000th time step in increments of 25 time steps (each time step is 1e-4 s). From 0.0s to 0.5s (i.e. 5000 iterations) Reynolds number (Re) was 58.3 that corresponds to incoming velocity of 0.5 m/s. The critical Re for a cylinder is about Re~40 when it starts exhibiting the von Karman wake instability. So the interval from 0 to 0.5 s at Re=58.3 corresponds to the Landau equation when the external input is greater than the bifurcation value. Then, starting at 0.5 seconds, the Re is being oscillated by oscillating incoming velocity. The oscillating Re corresponded to Re = 58.3 + 35*sin(2pi*omega*t), where omega corresponded to 2 Hz. The reason 35 was selected for the oscillating Re amplitude is because a large enough amplitude was needed such that the Re would oscillate above and below the critical value predicted by the regular Landau equation. The reason 2 Hz was selected is that it's an order of magnitude slower than the von Karman vortex frequency, which is about 39 Hz for Re = 58.3. Two simulations for the oscillating cylinder case were performed for the case of Re = 58.3 + 5.85*sin(2pi*omega*t) and Re = 58.3 + 1*sin(2pi*omega*t).

We used the following algorithm:

Let λ_j, j=1,2,..., 4969, be eigenvalues corresponding to Koopman Modes $V_{j,i}$, where j=1,2,...,4969, coordinates i=1,2,...,29954, for the stationary cylinder case. We find the Koopman Mode $V_{ind,i}$ from the stationary cylinder case that corresponds to the frequency of 39.26 Hz (Figure 19).

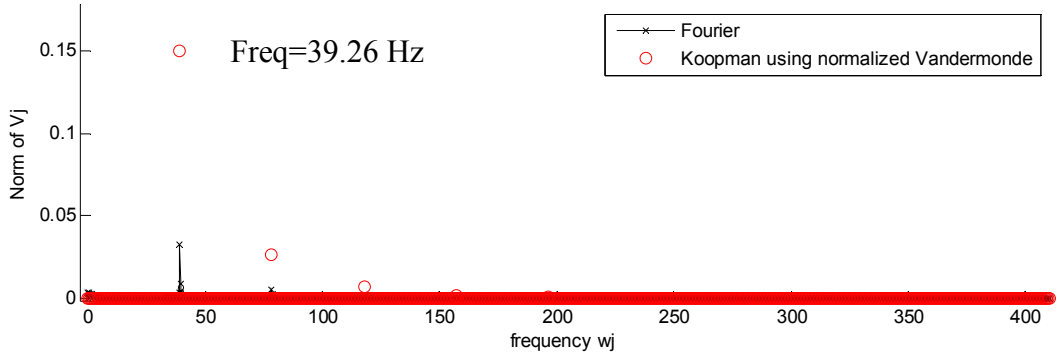

Figure 19. Fourier and KMD spectrum for u-velocity. FFT is in black; KM spectrum is red.

Then we find adjoint matrix B=(inv(V*V')*V)', that satisfies the condition that $[BV]_{k,k}=1$ and $[BV]_{k,l}=0$ for $k \neq l$.

Let X of size 4969x29954 be the u-velocity corresponding to the stationary cylinder.

Then we calculate $c_{ind,k}$ in the following way: for each k=1:size(B,1) for each i=1:size(X,1) we calculate $c_{ind,k}$(i,:)=dot(X(i,:),B(k,:))*V_{ind}(:). Then we find norm(abs($c_{ind,k}$)) (Figure 20).

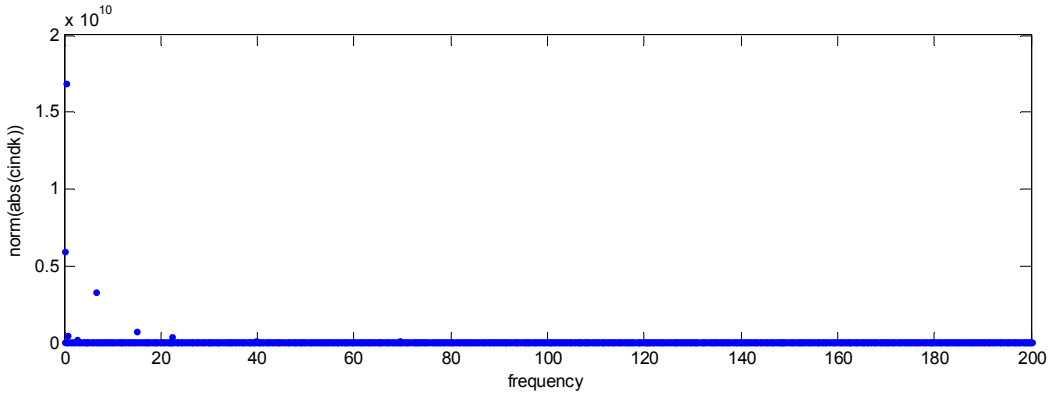

Figure 20. Norm of $c_{ind,k}$.

In Figure 22 we present $c_{ind,ind}$ vs simulation time and its embedding in time for w=39.26 Hz for Point 5 (Figure 21).

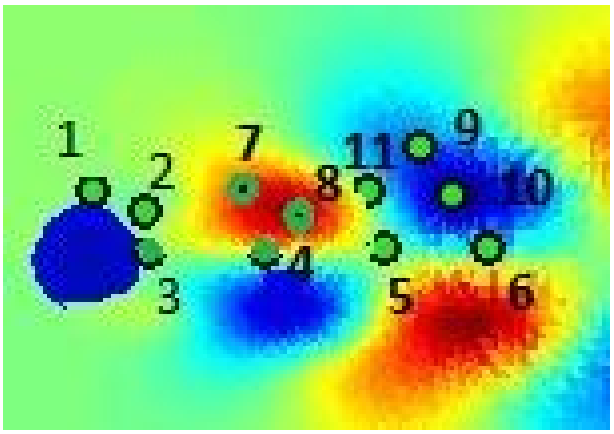

Figure 21. Points around the cylinder.

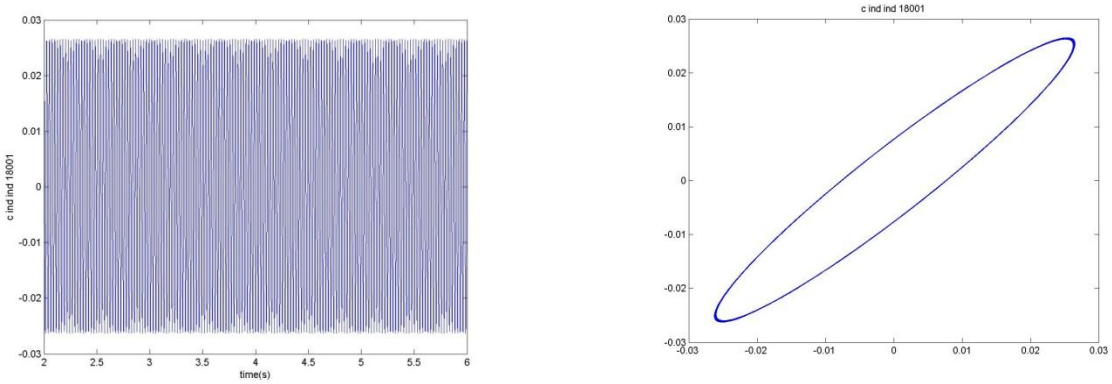

Figure 22. $c_{ind,ind}$ vs simulation time (left) and its embedding in time (right) for Point 5 for w=39.26 Hz.

We also calculate $c_{ind,k}$ for the oscillating cylinder cases by using the same algorithm as above with the difference that X of size 2400x29954 is the u-velocity corresponding to the oscillating cylinder case. In this case norm(abs($c_{ind,k}$)) is shown in Figures 23, 24 and 25.

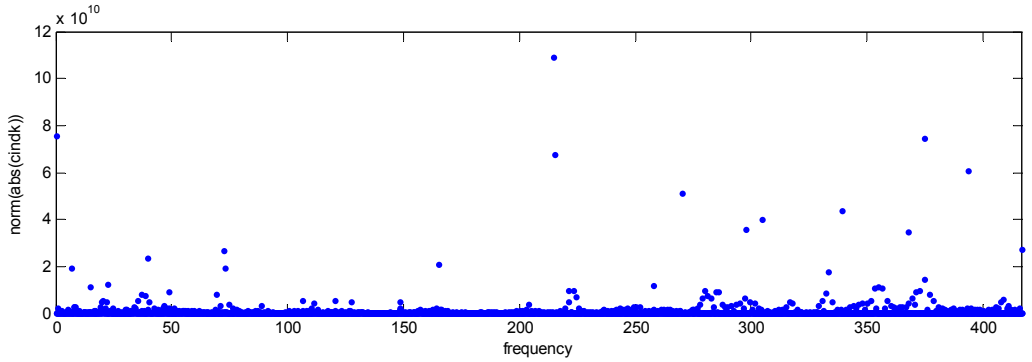

Figure 23. Norm of $c_{ind,k}$ for the oscillating cylinder case with Re=35.

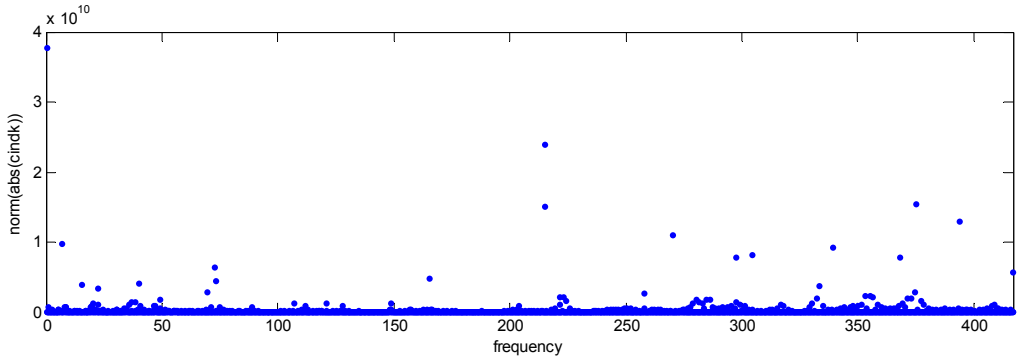

Figure 24. Norm of $c_{ind,k}$ for the oscillating cylinder case with Re=5.83.

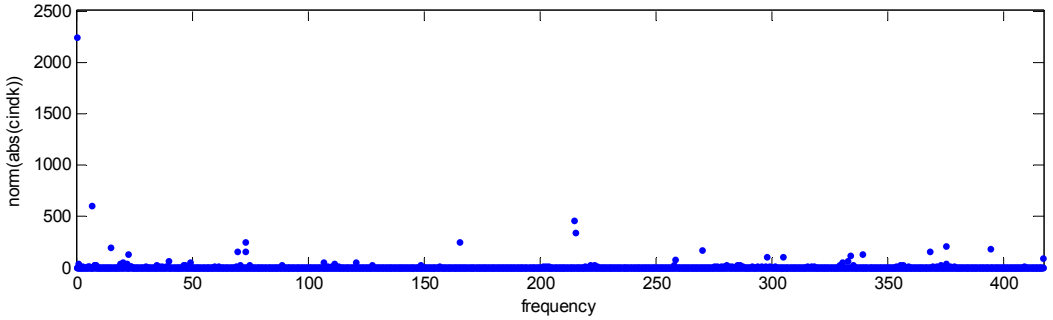

Figure 25. Norm of $c_{ind,k}$ for the oscillating cylinder case with Re=1.

In Figures 26, 27 and 28 we present $c_{ind,ind}$ vs simulation time and its embedding in time for Point 5 (Figure 21) for w=39.26 Hz for all oscillating cylinder cases.

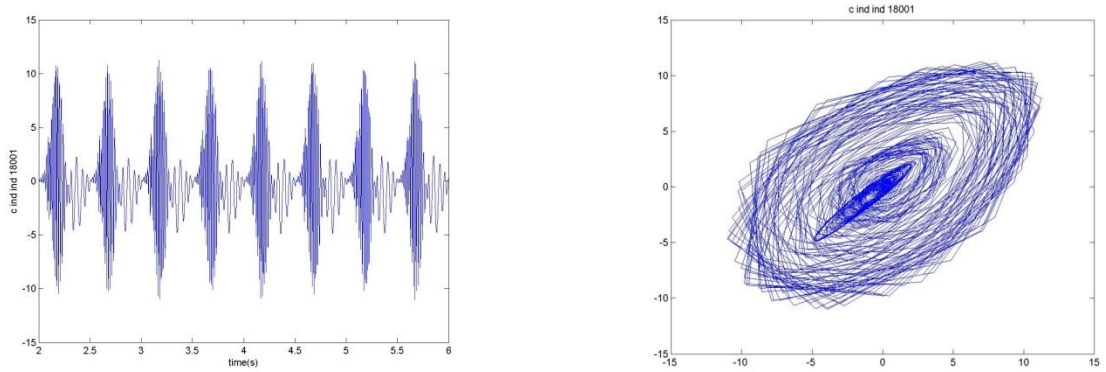

Figure 26. $c_{ind,ind}$ vs simulation time (left) and its embedding in time (right) for Point 5 for w=39.26 Hz for the oscillating cylinder case with Re=35.

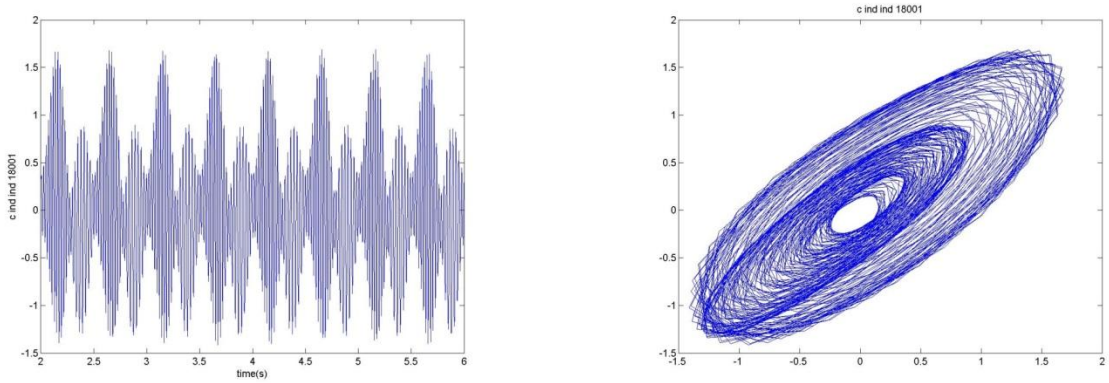

Figure 27. $c_{ind,ind}$ vs simulation time (left) and its embedding in time (right) for Point 5 for w=39.26 Hz for the oscillating cylinder case with Re=5.83.

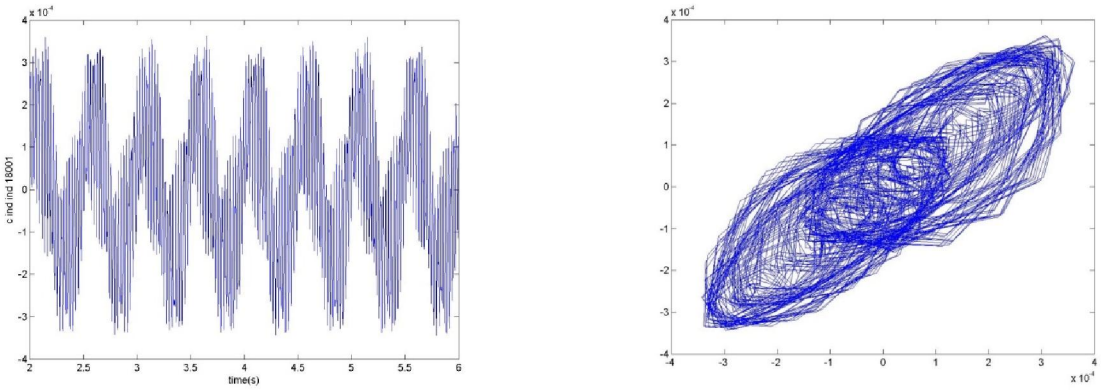

Figure 28. $c_{ind,ind}$ vs simulation time (left) and its embedding in time (right) for Point 5 for w=39.26 Hz for the oscillating cylinder case with Re=1.

Koopman mode projections of cylinder in oscillating inlet flow show an interesting transition that happens with the increase of Reynolds number. Specifically, the spectrum is strongly peaked at low Reynolds number, and shows continuous elements as Reynolds number increases. The transition starts with broadening of the spectrum around harmonics of vortex shedding frequency

and leads to merging of spectrum into a continuous-looking spectrum at higher Reynolds numbers. We researched connections of these transitions to normal form equations that extend those obtained for Hopf bifurcation. We found that adding a constant forcing term to the Hopf bifurcation normal form, along the lines suggested by the paper of [Tsarouhas: 1987] does not lead to a good match with observed transition in the fluid-mechanical problem. Further investigation lead to suggestion of adding a term proportional to the radial coordinate in the normal form, similar to the suggestion made in papers of Young and collaborators (2003, 2008). This approach proved very promising, with spectral results matching closely the progression of spectral changes in the flow, especially around shedding frequency. The normal form model, however, does not match the spectrum at the inlet flow oscillating frequency. Our conjecture is that this might be due to absence of pure (radial coordinate independent) oscillating term in the current version of the normal form.

Conclusions

We believe that the given study can be extended to capture aspects of a number of different applied problems of Army interest in flow-structure interaction, where the flow affecting the structure is unsteady or the structure is moving in an unsteady manner.

References

[Ham:1968] Norman D Ham and Melvin S Garelick. Dynamic stall considerations in helicopter rotors. Journal of the American Helicopter Society, 13(2):49-55, 1968.
[Johnson:1972] Wayne Johnson and Norman D Ham. On the mechanism of dynamic stall. Journal of the American Helicopter Society, 17(4):36-45, 1972.
[Barwey:1994] Dinesh Barwey and Gopal H Gaonkar. Dynamic-stall and structural-modeling effects on helicopter blade stability with experimental correlation. AIAA journal, 32(4):811-819, 1994.
[Holmes: 1998] P. Holmes, J.L. Lumley, and G. Berkooz. Turbulence, coherent structures, dynamical systems and symmetry. Cambridge Univ. Press, 1998.
[Mccroskey:1982] WJ McCroskey. Unsteady airfoils. Annual Review of Fluid Mechanics, 14(1):285-311, 1982.
[Carr:2012] L.W. Carr. Progress in analysis and prediction of dynamic stall. Journal of Aircraft, 25(1), 2012.
[Ekaterinaris:1998] J.A. Ekaterinaris and M.F. Platzer. Computational prediction of airfoil dynamic stall. Progress in aerospace sciences, 33(11-12):759-846, 1998.
[Mezic: 2005] I. Mezic. Spectral properties of dynamical systems, model reduction and decompositions. Nonlinear Dynamics, 41(1):309-325, 2005.
[Koopman: 1931] B.O. Koopman. Hamiltonian systems and transformation in Hilbert space. Proceedings of the National Academy of Sciences of the United States of America, 17(5):315, 1931.

[Schmid: 2008] P. Schmid and J. Sesterhenn. Dynamic mode decomposition of numerical and experimental data. 61st Annual Meeting of the APS Division of Fluid Dynamics, November 2008.
[Rowley: 2009] C.W. Rowley, I. Mezic, S. Bagheri, P. Schlatter, and D.S. Henningson. Spectral analysis of nonlinear flows. Journal of Fluid Mechanics, 641(1):115-127, 2009.
[Plonka: 2014] Gerlind Plonka, Manfred Tasche, Prony Methods for Recovery of Structured Functions, GAMM-Mitteilungen, 3 June 2014
[Bagheri: 2013] Shervin Bagheri, Koopman-mode decomposition of the cylinder wake, J. Fluid Mech. (2013), vol. 726, pp. 596-623, doi:10.1017/jfm.2013.249
[Vance: 1989] William Vance, George Tsarouhas and John Ross, Universal Bifurcation Structures of Forced Oscillators, Progress of Theoretical Physics Supplement No. 99, 1989, pp.331-338
[Wang: 2003] Qiudong Wang, Lai-Sang Young, Strange Attractors in Periodically-Kicked Limit Cycles and Hopf Bifurcations, Commun. Math. Phys. 240, 509–529 (2003), Digital Object Identifier (DOI) 10.1007/s00220-003-0902-9
[Lin: 2008] Kevin K Lin, Lai-Sang Young, Shear-induced chaos, Nonlinearity 21 (2008) 899–922, doi:10.1088/0951-7715/21/5/002
[Tsarouhas: 1987] Tsarouhas, George E., and John Ross. "Explicit solutions of normal form of driven oscillatory systems." *The Journal of chemical physics* 87.11 (1987): 6538-6543
[Young: 2003] Wang, Qiudong, and Lai-Sang Young. "Strange attractors in periodically-kicked limit cycles and Hopf bifurcations." *Communications in mathematical physics* 240.3 (2003): 509-529
[Young: 2008] Lin, Kevin K., and Lai-Sang Young. "Shear-induced chaos." *Nonlinearity* 21.5 (2008): 899